Iron-sulfur cluster repair contributes to *Y. pseudotuberculosis* survival within deep tissues.

Running title: Iron-sulfur cluster repair during *Y. pseudotuberculosis* infection

Kimberly M. Davis[1,#a,*], Joanna Krupp[1], Stacie Clark[1,2], Ralph R. Isberg[1]

[1]Department of Molecular Biology and Microbiology
[2]Graduate Program in Molecular Microbiology
Tufts University School of Medicine, Boston, MA, USA
[#a]Current Address: W. Harry Feinstone Department of Molecular Microbiology and Immunology
Johns Hopkins Bloomberg School of Public Health, Baltimore, MD, USA

*Corresponding author:

E-mail: kdavi140@jhu.edu (KMD)

Abstract

To successfully colonize host tissues, bacteria must respond to and detoxify many different host-derived antimicrobial compounds, such as nitric oxide (NO). NO has direct antimicrobial activity through attack on iron-sulfur (Fe-S) cluster-containing proteins. NO detoxification plays an important role in promoting bacterial survival, but it remains unclear if repair of Fe-S clusters is also important for bacterial survival within host tissues. Here we show that the Fe-S cluster repair protein, YtfE, contributes to the survival of *Y. pseudotuberculosis* within the spleen following nitrosative stress. *Y. pseudotuberculosis* forms clustered centers of replicating bacteria within deep tissues, where peripheral bacteria express the NO-detoxifying gene, *hmp*. *ytfE* expression also occurred specifically within peripheral cells at the edges of microcolonies. In the absence of *ytfE*, the area of microcolonies was significantly smaller than WT, consistent with *ytfE* contributing to the survival of peripheral cells. The loss of *ytfE* did not alter the ability of cells to detoxify NO, which occurred within peripheral cells in both WT and Δ*ytfE* microcolonies. In the absence of NO-detoxifying activity by *hmp*, NO diffused across Δ*ytfE* microcolonies, and there was a significant decrease in the area of microcolonies lacking *ytfE*, indicating that *ytfE* also contributes to bacterial survival in the absence of NO detoxification. These results indicate a role for Fe-S cluster repair in the survival of *Y. pseudotuberculosis* within the spleen, and suggest that extracellular bacteria may rely on this pathway for survival within host tissues.

44 **Introduction**

45 Nitric oxide (NO) is a diffusible gas that has a wide range of physiological functions
46 within mammals (1, 2). The effects of NO are tissue concentration-dependent, as it promotes
47 vasodilation, cell proliferation and cell differentiation at low concentrations (3, 4), while high
48 concentrations drive apoptosis and defense against bacterial, fungi, and parasites (5-8). NO is
49 produced by three different nitric oxide synthase (NOS) isoforms within mammalian tissues: the
50 neuronal NOS (nNOS), endothelial NOS (eNOS), and inducible NOS (iNOS). nNOS and eNOS
51 are expressed at low levels by endothelial and neuronal cells respectively (2). In contrast, iNOS
52 is expressed by a wide range of cell types, specifically in response to NF-κB-dependent sensing
53 of, and is responsible for the high levels of NO produced during infection (1, 9).

54 NO has direct antimicrobial activity and can also react with reactive oxygen species to
55 produce additional toxic compounds, such as peroxynitrite. NO may be bacteriostatic, while
56 peroxynitrite is known to have direct bactericidal activity (10). NO antibacterial activity occurs
57 through nitrosylation of iron-sulfur (Fe-S) cluster-containing proteins, which play critical roles in
58 cellular respiration, DNA synthesis, and gene regulation. NO also targets heme groups, reactive
59 thiols, tyrosyl radicals, and can cause DNA damage (1, 10). One of the global regulators in *E.*
60 *coli* that has been shown to be inactivated by NO is NsrR (11), which regulates the response to
61 nitrosative stress and is also associated with the oxidative stress response (12-14). Nitrosylation
62 of the NsrR-associated Fe-S cluster relieves repression of at least 60 genes in *E. coli* (15-18).
63 Included in this regulon is the *hmp* gene, which encodes a flavohemoglobin that detoxifies NO
64 (19, 20), and YtfE (also known as Repair of Iron Centers (RIC) in *E. coli*), which functions to
65 repair Fe-S clusters following NO damage (13, 17). Repair of Fe-S cluster proteins by YtfE can
66 eliminate the need for new Fe-S cluster biogenesis when Fe availability is limited (13, 21, 22). A

67 variety of studies argue that YtfE contributes to bacterial survival within host cells, but it remains
68 unclear if YtfE contributes to the survival of extracellular pathogens replicating within host
69 tissues, and if YtfE contributes to survival following exposure to NO (23-25).

70 *Yersinia pseudotuberculosis* is an oral pathogen that is typically contained within
71 intestinal tissues and gut-associated lymphoid tissues, but has the capacity to spread systemically
72 in susceptible individuals (26-29). Following bloodstream access, *Y. pseudotuberculosis*
73 colonizes deep tissue sites where individual bacteria replicate to form clonal microcolonies (30-
74 32). Neutrophils, monocytes, and macrophages are recruited to sites of bacterial replication,
75 which are kept at bay by *Yersinia*, primarily via substrates of the bacterial type III secretion
76 system (33-35). Recruited monocytes and macrophages produce NO, which diffuses across a
77 layer of neutrophils and is inactivated at the periphery of the microcolony by bacteria expressing
78 Hmp, preventing diffusion of NO into the interior of the microcolony (32). The consequences of
79 the selective attack of NO on the peripheral bacteria are unclear, although it is likely that
80 nitrosative stress may slow their growth. Additional members of the nitrosative stress response,
81 such as YtfE, may also be required in peripheral cells to ensure their survival.

82 Bacteria responding to RNS appear to recover and remain viable, consistent with
83 members of the NsrR regulon cooperating to repair NO-mediated damage in peripheral bacteria
84 within microcolonies. Two of the members of the *E. coli* NsrR regulon, *hmp* and *ytfE,* are
85 upregulated in the bubonic plague model of *Yersinia pestis* infection and during Peyer's patch
86 colonization by *Y. pseudotuberculosis* (36, 37). The similar expression patterns of *hmp* and *ytfE*
87 may suggest that both genes are also members of the NsrR regulon in *Yersinia,* and could both
88 contribute to microbial fitness during microcolony growth. Additionally, very few studies have
89 explored the role of Fe-S cluster repair during infection with extracellular bacteria. Here, we

90 show that *ytfE* contributes to the survival of extracellular bacteria, specifically through

91 upregulation of *ytfE* within peripheral cells of *Y. pseudotuberculosis* microcolonies.

92 **Results.**

93 ***Y. pseudotuberculosis ytfE* expression is regulated by NsrR and occurs within peripheral**
94 **cells during growth in the spleen.**

95 The *ytfE* gene is known to be a member of the NsrR regulon in a number of bacterial
96 species (13, 14, 38), so *ytfE* is expected to be repressed by NsrR in *Y. pseudotuberculosis*. We
97 also expected that *ytfE* is transcribed during *Y. pseudotuberculosis* growth within the mouse
98 spleen as the NsrR-regulated *hmp* gene is expressed in this tissue (23-25, 32, 36). To determine if
99 *Y. pseudotuberculosis ytfE* is expressed during splenic growth, C57BL/6 mice were intravenously
100 challenged with bacteria and bacterial RNA was isolated at day 3 post-inoculation (PI). Based on
101 qRT-PCR analysis, *ytfE* transcript levels increased within the mouse spleen relative to the
102 inoculum culture grown in the absence of an NO-generating system, with marked mouse-to-
103 mouse variation (Figure 1A) (32). To determine if *ytfE* expression is NsrR-dependent, we
104 compared *ytfE* transcription levels in WT and Δ*nsrR* strains in the presence (+) and absence (-) of
105 nitrogen stress imparted by acidified nitrite (NO_2). Transcription of *ytfE* increased by over 100X
106 in the WT strain with the addition of nitrogen stress (Figure 1B). Transcription of *ytfE* was high
107 in the Δ*nsrR* strain in either the presence or absence of nitrogen stress, indicating that NsrR
108 negatively regulates *ytfE* transcription. A slight increase in *ytfE* expression in the Δ*nsrR* strain
109 with nitrogen stress suggests additional pathways may regulate *ytfE* expression.

110 Hmp, another member of the NsrR regulon, is specifically expressed on the periphery of
111 *Y. pseudotuberculosis* microcolonies during splenic growth (32). At the transcriptional level,
112 this is associated with considerable variation in expression levels between individual mice.
113 Variation is likely due to the presence of different size microcolonies within different organs, as
114 distinct peripheral expression of *hmp* is visualized in large microcolonies, and smaller

115 microcolonies are more homogenous. The variable *ytfE* expression levels in the mouse and
116 NsrR-dependence is reminiscent of *hmp* expression, indicating that there could be a link between
117 spatial expression and inter-mouse variation. To determine if *ytfE* and *hmp* have similar
118 expression patterns during growth in the spleen, mice were intravenously inoculated with a WT
119 *Y. pseudotuberculosis* strain containing *hmp::mCherry* (chromosomal integration of *mCherry*
120 downstream of *hmp*) and *ytfE::gfp* (chromosomal integration of *gfp* downstream of *ytfE*).
121 Microcolonies were visualized within the spleen using fluorescence microscopy, and *ytfE* and
122 *hmp* reporter signals were quantified within the same cells at the center and periphery of the
123 microcolonies (Materials and Methods). The *hmp* reporter signal increased within individual
124 cells at the periphery relative to cells at the centroid of microcolonies, which generated a ratio
125 value greater than 1, consistent with *hmp* peripheral expression (Figure 1C). The *ytfE* signal was
126 dim relative to *hmp*, but also increased at the periphery of microcolonies relative to the centroid.
127 The Periphery/Centroid signal intensity ratio value for *ytfE* was similar to *hmp*, indicating that
128 *ytfE* was expressed at the periphery of microcolonies (Figure 1C). To confirm the dim *ytfE*
129 signal was not due to mCherry fluorescence detected in the gfp channel, experiments were also
130 performed in a WT strain containing *yopE::mCherry* and *ytfE::gfp*. *yopE* and *ytfE* exhibited
131 distinct reporter patterns indicating the detected gfp signal was due to *ytfE* reporter expression
132 (Figure 1C, 1D). There was significant overlap in the *hmp* and *ytfE* signals within these images,
133 and based on NsrR-dependent regulation of both genes, it is likely that *hmp* and *ytfE* were
134 expressed in the same cells (Figure 1D).

135 ***ytfE* contributes to the virulence of *Y. pseudotuberculosis* in the spleen.**

136 YtfE repairs Fe-S clusters damaged by NO, and there appears to be sufficient NO at the
137 periphery of splenic microcolonies to allow synthesis of this protein and to promote repair within

138 this subpopulation of bacteria. To determine if loss of *yftE* alters the overall fitness of *Y.*
139 *pseudotuberculosis* during growth within the spleen, we constructed a *Y. pseudotuberculosis*
140 strain that lacks the *ytfE* gene (Δ*ytfE*) and harbors a constitutive *gfp*-expressing plasmid, to
141 visualize growth within the spleen. To compare differences in relative fitness, mice were
142 infected intravenously with equal amounts of WT mCherry$^+$ and Δ*ytfE* GFP$^+$ strains, and spleens
143 were harvested at day 3 PI, a late stage of infection in this model, to determine the competitive
144 index by colony forming units (CFUs) and quantify microcolony areas within the same animals.
145 At day 3 PI, the median competitive index was significantly less than 1, indicating lowered
146 fitness of the Δ*ytfE* strain relative to the WT strain (Figure 2A; p=0.0115). The areas of
147 individual microcolonies within these co-infected tissues were also visualized and quantified by
148 fluorescence microscopy in 11 mice. The Δ*ytfE* microcolonies were significantly smaller than
149 WT microcolonies within the same organs, indicating that *ytfE* contributes to the survival of *Y.*
150 *pseudotuberculosis* in the spleen, presumably due to lowered fitness of the bacterial population
151 located at the periphery of the microcolonies (Figure 2B).
152 Since YtfE could directly repair the Fe-S cluster of NsrR, the absence of *ytfE* could alter
153 expression of the NsrR regulon, by resulting in heightened expression within peripheral cells. To
154 determine if microcolonies from the *Y. pseudotuberculosis* Δ*ytfE* strain have sustained
155 expression of the NsrR regulon relative to the WT strain, we infected mice intravenously with
156 WT GFP$^+$ *hmp::mCherry* or Δ*ytfE* GFP$^+$ *hmp::mCherry* integrated *hmp* reporter strains, and
157 spleens were harvested at day 3 PI to visualize reporter expression by fluorescence microscopy.
158 Similar to Fig. 1D, *hmp* reporter expression was significantly higher at the periphery relative to
159 the centroid in the WT strain (Figure 2C). The reporter expression pattern was very similar in
160 Δ*ytfE* microcolonies, indicating that there was still a gradient of NO exposure in the mutant, in

161 which Hmp activity in the peripheral population protects the central population of bacteria, and
162 that loss of *ytfE* did not significantly alter expression of the NsrR regulon (Figure 2D).

163 ***ytfE* contributes to bacterial survival in the absence of *hmp*.**

164 YftE contributed to the growth of *Y. pseudotuberculosis* microcolonies in the spleen
165 despite expression limited to the microcolony periphery. We were then interested in determining
166 if YtfE-mediated repair played an important role in the context of a Δ*hmp* strain, where all
167 bacteria in a microcolony are exposed to NO (32). To address this point, we challenged mice
168 intravenously with Δ*hmp* GFP$^+$ P_{hmp}*::mCherry* and Δ*hmp* Δ*ytfE* GFP$^+$ P_{hmp}*::mCherry* strains, and
169 spleens were harvested at day 3 PI to quantify CFUs, visualize microcolony areas, and detect
170 reporter signals by fluorescence microscopy. The Δ*hmp* Δ*ytfE* strain showed no potentiation of
171 the defect in single strain infections, but this defect can be observed during co-infection. The
172 median competitive index (CI) value for the double mutant was below 1, but was not
173 significantly less than 1, which suggests that Δ*hmp* Δ*ytfE* strain may not be less fit than Δ*hmp*
174 (Figure 3A). Interestingly, in 4 mice the CI was at least 1, indicating that the Δ*hmp* Δ*ytfE* strain
175 could compete efficiently with Δ*hmp* in these animals. We then compared the total CFU in the
176 organs in mice in which the Δ*hmp* strain outcompeted Δ*hmp* Δ*ytfE*, or in mice in which no such
177 outcompetition took place (Figure 3B). The total CFUs were significantly lower in organs in
178 which the Δ*hmp* did not outcompete the Δ*hmp*Δ*ytfE* strain, indicating that the fitness differences
179 were suppressed in animals showing increased restriction of bacterial growth. It is also possible
180 that the Δ*hmp*Δ*ytfE* strain had reduced levels of initial seeding within tissues. The microcolony
181 areas were quantified within all the spleens depicted in Figure 3A, and the areas of Δ*hmp* Δ*ytfE*
182 microcolonies were significantly smaller than Δ*hmp* (Figure 3C). Δ*hmp* Δ*ytfE* microcolonies had
183 similar P_{hmp} reporter expression at the centroid and periphery, indicating NO diffused across

184 these centers (Figure 3D). Together, these results confirm that *ytfE* contributes to bacterial
185 survival in the absence of Hmp detoxifying activity.

186 **_ytfE_ has limited effects on NO sensitivity in the absence of _hmp_**

187 The Δ*ytfE* single mutant strain had reduced fitness relative to the WT strain (Figure 2),
188 however the single Δ*ytfE* mutant was not significantly more sensitive than the WT strain to the
189 presence of acidified nitrite during growth in culture. Similarly, despite the lowered fitness of the
190 Δ*hmp* Δ*ytfE* strain in spleens relative to Δ*hmp*, the Δ*hmp* Δ*ytfE* strain was not significantly more
191 sensitive than the Δ*hmp* mutant strain to the presence of acidified nitrite during growth in culture
192 (Figure 4A; compare +NO_2 samples). The absence of *ytfE* also did not significantly alter the
193 sensitivity of strains to the NO donor compound, DETANONOate, during growth in minimal
194 media (Figure 4B). This is consistent with previous reports in other organisms (38, 39), perhaps
195 due to the presence of other backup repair pathways that are active in the absence of Hmp or
196 because YtfE plays a role in protection from other stress species.

197 We then compared *hmp* reporter expression in Δ*ytfE* and Δ*hmp*Δ*ytfE* strains to confirm
198 that NO diffusion occurred across Δ*hmp* Δ*ytfE* microcolonies using plasmid-borne reporters.
199 Mice were infected intravenously with Δ*ytfE* GFP^+ P_{hmp}*::mCherry* or Δ*hmp* Δ*ytfE* GFP^+
200 P_{hmp}*::mCherry* strains, and spleens were harvested 3 days PI to visualize reporter expression by
201 fluorescence microscopy. The Δ*ytfE* strain had peripheral P_{hmp} reporter expression, as seen with
202 the chromosomally-integrated *hmp* reporter, indicating that NO diffusion across the microcolony
203 is inhibited by peripheral cells in Δ*ytfE* microcolonies (Figure 4C, 4D). Δ*hmp* Δ*ytfE*
204 microcolonies showed no such preference for the periphery, indicating NO diffused across these
205 centers, as expected based on the loss of *hmp*.

206 **Rescue of _ytfE_ restores microcolony size.**

207 To show that the loss of *ytfE* was responsible for decreased microcolony size, we rescued
208 the Δ*ytfE* strain with a WT copy of *ytfE*, and transformed the *ytfE* rescued strain with the
209 constitutive *gfp*-expressing plasmid. Mice were infected intravenously with WT mCherry$^+$ and
210 *ytfE* rescued GFP$^+$ strains, and spleens were harvested at day 3 PI to quantify CFUs and visualize
211 microcolony areas by fluorescence microscopy. The median competitive index for the *ytfE*
212 rescued strain was close to a value of 1, indicating the fitness of this strain was roughly
213 equivalent to the WT strain (Figure 5A). The microcolony areas were quantified within all the
214 spleens depicted in Figure 5A, and the areas of *ytfE* rescued microcolonies were very similar to
215 WT microcolonies (Figure 5B, 5C). These results indicate that the Δ*ytfE* strain was rescued by
216 the WT copy of *ytfE*, which confirms that the reduced fitness of the Δ*ytfE* strain was specifically
217 due to a loss of *ytfE.*

218 **Discussion**

219 The detoxification of NO and other reactive nitrogen species is critical for bacterial
220 survival within host tissues (40-43). Bacterial proteins involved in NO detoxification, however,
221 are not synthesized until NO accumulates and damages the Fe-S clusters of NsrR, resulting in
222 inactivation of this repressor (15, 16). Many additional Fe-S cluster-containing proteins are
223 simultaneously damaged, so bacteria need to either repair damaged proteins or synthesize
224 replacement proteins, while simultaneously replenishing proteins that detoxify NO and prevent
225 further damage (17, 38). Although Fe-S cluster repair is likely required for bacterial survival, it
226 has been unclear whether or not this plays an important role within host tissues. We have chosen
227 to ask this question in a mouse model of *Y. pseudotuberculosis* infection, where it is known that
228 bacteria respond to RNS and that Fe concentrations are limiting (24, 25, 32). *ytfE* expression
229 had been detected in *Yersinia* species replicating within host tissues, however it was unclear if
230 Fe-S cluster repair or assembly play a significant role during infection (36, 37). Here, we have
231 shown that Fe-S cluster repair contributes to successful *Y. pseudotuberculosis* replication within
232 the spleen.

233 We found that a place where Fe-S cluster repair in *Y. pseudotuberculosis* likely occurs is
234 in the peripheral subpopulation of bacteria that responds to NO assault within microcolonies.
235 This is consistent with a role for YftE in supporting survival of the peripheral subpopulation. In
236 the absence of *ytfE*, we would expect bacteria on the periphery to be exposed to stress associated
237 with NO exposure, leading to sequential loss of the peripheral population and progressively
238 smaller microcolonies. Consistent with this hypothesis, we observed Δ*ytfE* microcolonies were
239 smaller than those established by the WT strain. It is expected that the difference between WT
240 and Δ*ytfE* microcolony areas will become progressively more pronounced as the infection

241 proceeds, because Δ*ytfE* microcolonies should continuously lose their peripheral subpopulation.
242 This prediction is based on our previous observation that NO-sensitive microcolonies are
243 progressively reduced during the course of disease, with elimination of Δ*hmp* bacteria by NO
244 most pronounced at late timepoints post-inoculation, concurrent with a timepoint in which the
245 animals inoculated with the WT strain are moribund (32).

246 NO alone was not sufficient to limit the growth of Δ*ytfE* bacteria in bacteriological
247 media, consistent with previous studies that indicated the uropathogenic *E. coli* (UPEC) Δ*ytfE*
248 strain had reduced intracellular survival within host cells, but was not sensitive to exogenous NO
249 alone (39). Presumably, the Δ*ytfE* strain is sensitive to other antimicrobial compounds generated
250 within host tissues, possibly by the generation of a variety of reactive nitrogen species (RNS) as
251 a consequence of NO reaction with reactive oxygen species (ROS) or other compounds.
252 Upregulation of *ytfE* following hydrogen peroxide-mediated damage of *Staphylococcus aureus*
253 indicates that YtfE may play a broad role in repair, instead of just a response to nitrogen stress
254 (44, 45). Additional studies in *E. coli* also suggest that YtfE repairs Fe-S cluster proteins
255 damaged by hydrogen peroxide (13, 46-49).

256 An additional regulatory signal for the *yftE* gene is iron limitation, which depresses
257 synthesis of new Fe-S cluster proteins, thus requiring cellular YftE function (14, 21, 50). The
258 spleen is expected to be an iron-limiting environment requiring Fe-S cluster repair, but we found
259 no evidence for NO-independent induction of the *ytfE* gene within the center of microcolonies,
260 using our fluorescent promoter constructions. This contrasts with data arguing that *Y.*
261 *pseudotuberculosis* expresses many Fe acquisition genes during growth in host tissues, consistent
262 with Fe-limiting conditions within host tissues (25, 37). It is possible that the center of the
263 microcolony represents a protected environment with low exposure to stresses such as reactive

264 nitrogen and oxygen species as well as limited damage to Fe-S centers. Additionally, *ytfE*
265 expression may be induced at very low NO concentrations, as seen in *Salmonella enterica*
266 serovar Typhimurium (38), but may require severe iron limitation for expression in the absence
267 of NO.

268 The loss of YftE function also has the potential to alter metabolite levels due to
269 disruption of protein functions that are Fe-S center-related. In the presence of RNS, a Δ*ytfE*
270 strain may have reduced aconitase and fumarase activity due to the role of YtfE in Fe-S cluster
271 repair specifically for these proteins (47). The Fe-S cluster of the NsrR repressor is also repaired
272 by YtfE, which could lead to prolonged expression of the NsrR regulon in the presence of NO
273 (13). Our results indicate that expression of the NsrR regulon is similar in the presence or
274 absence of *ytfE*, although it remains possible that prolonged expression of the NsrR regulon
275 could be detected at later timepoints post-inoculation. Future work will investigate these issues,
276 and determine the interplay between iron regulation, NO-induced damage and repair of critical
277 Fe-S centers.

278 **Materials and Methods**

279 *Bacterial strains & growth conditions.* The WT *Y. pseudotuberculosis* strain, YPIII, was
280 used throughout. For all mouse infection experiments, bacteria were grown overnight to post-
281 exponential phase in 2xYT broth (LB, with 2x yeast extract and tryptone) at 26° C with rotation.
282 Exponential phase cultures were sub-cultured 1:100 from overnight cultures, and grown at 26° C
283 with rotation for an additional 2 hours. Sodium nitrite (2.5mM) was added to LB pH5.5 to
284 induce the nitrogen stress response. DETA-NONOate (2.5mM) NO donor compound (Cayman
285 Chemicals) was added to M9 minimal media to test NO sensitivity.

286 *Generation of ytfE mutant strains.* The *hmp* and *nsrR* deletion strains were previously
287 described (32). Deletion derivative strains were generated for *ytfE* by amplifying the start codon
288 + 3 downstream codons, the 3' terminal 3 codons + the stop codon and fusing these fragments to
289 generate a start + 6 aa + stop construct. Deletion constructions were amplified with 500 base
290 pairs flanking sequence on each side, cloned into the suicide vector, pSR47S, and transformed
291 into *Y. pseudotuberculosis*. Sucrose selection was used to select for bacteria that had
292 incorporated the desired mutation after a second cycle of recombination (31). PCR, sequencing,
293 and qRT-PCR were used to confirm deletion strains.

294 *Integrated ytfE reporter construction (ytfE^{+}rescue strain).* The *ytfE::gfp* reporter was
295 generated by cloning *gfp* immediately downstream of the *ytfE* gene (in between the *ytfE* stop
296 codon and terminator sequence) by overlap extension PCR. The *ytfE* start codon was amplified
297 with 500 base pairs upstream flanking sequence, while the stop codon of *gfp* was amplified with
298 500 base pairs downstream flanking sequence. This fragment was cloned into the suicide vector,
299 pSR47S, and transferred by conjugation into WT *Y. pseudotuberculosis hmp::mCherry*
300 (chromosomally integrated), selecting for kanamycin resistance. For the *ytfE*$^{+}$ rescue strain, a

301 WT *ytfE* gene product, including 500 base pairs upstream and downstream of *ytfE*, was amplified
302 from genomic DNA and cloned into pSR47S. This vector was transferred by conjugation into
303 Δ*ytfE Y. pseudotuberculosis*, selecting for kanamycin resistance. A second round of
304 recombination was selected on sucrose-containing media to isolate strains that had recombined
305 each *ytfE* construct. PCR and sequencing were used to confirm integration of *gfp* or rescue of
306 the *ytfE* deletion.

307 *Generation of plasmid-based reporter strains.* Several of the *Y. pseudotuberculosis*
308 reporter strains in this study have been previously described: WT GFP^+, WT $mCherry^+$
309 (*yopE::mCherry)*, WT *hmp::mCherry*, WT GFP^+ *hmp::mCherry*, and Δ*hmp* GFP^+ (32). For this
310 study, GFP^+ strains were constructed by transforming deletion strains with the constitutive GFP
311 plasmid, which expresses GFP from an unrepressed P_{tet} of pACYC184. The P_{hmp}*::mCherry* was
312 also transformed into GFP^+ strains. The P_{hmp}*::mCherry* transcriptional fusion was previously
313 constructed by fusing the *hmp* promoter to *mCherry* using overlap extension PCR, and cloned
314 into the pMMB67EH plasmid (32).

315 *Murine model of systemic infection.* Six to 8-week old female C57BL/6 mice were
316 obtained from Jackson Laboratories (Bar Harbor, ME). All animal studies were approved by the
317 Institutional Animal Care and Use Committee of Tufts University. Mice were injected
318 intravenously with 10^3 bacteria for all experiments. For co-infection experiments, mice were
319 inoculated with 5 x 10^2 CFU of each strain, for a total of 10^3 CFUs. At the indicated timepoints
320 post-inoculation (PI) (3 days), spleens were removed and processed.

321 *qRT-PCR to detect bacterial transcripts in broth-grown cultures.* Bacterial cells were
322 grown in broth to A_{600} = 0.3 under appropriate stress conditions, pelleted, resuspended in Buffer
323 RLT (QIAGEN) + ß-mercaptoethanol, and RNA was isolated using the RNeasy kit (QIAGEN)

324 according to manufacturer's protocol. DNA contamination was eliminated using the DNA-free
325 kit (Ambion) according to manufacturer's protocol. RNA was reverse transcribed using M-MLV
326 reverse transcriptase (Invitrogen), in the presence of the RNase inhibitor, RnaseOUT
327 (Invitrogen), according to manufacturer's protocol. Approximately 30 ng cDNA was used as a
328 template in reactions with 0.5 μM of forward and reverse primers and SYBR Green (Applied
329 Biosystems) according to manufacturer's protocol. Control samples were prepared that lacked
330 M-MLV, to confirm DNA was eliminated from samples and was not amplified by qRT-PCR.
331 Reactions were carried out using the StepOnePlus Real-Time PCR system, and relative
332 comparisons were obtained using the $\Delta\Delta C_T$ or $2^{-\Delta Ct}$ method (Applied Biosystems).
333 *qRT-PCR to detect bacterial transcripts from mouse tissues.* Mice were inoculated
334 intravenously with the WT strain, and at day 3 PI spleens were harvested, and immediately
335 submerged in RNALater solution (QIAGEN). Tissue was homogenized in Buffer RLT + ß-
336 mercaptoethanol, and RNA was isolated using the RNeasy kit (QIAGEN) according to
337 manufacturer's protocol. Bacterial RNA was enriched following depletion of host mRNA and
338 rRNA from total RNA samples, using the MICROB*Enrich* kit (Ambion) according to
339 manufacturer's protocol. DNA digestion, reverse transcription, and qRT-PCR were performed
340 as described above.
341 *Fluorescence microscopy.* C57BL/6 mice were inoculated intravenously with the *Y.*
342 *pseudotuberculosis* WT strain, at day 3 PI spleens were harvested and immediately fixed in 4%
343 paraformaldehyde in PBS for 3 hours. Tissues were frozen-embedded in Sub Xero freezing
344 media (Mercedes Medical) and cut by cryostat microtome into 10μm sections. To visualize
345 reporters, sections were thawed in PBS, stained with Hoechst at a 1:10,000 dilution, washed in
346 PBS, and coverslips were mounted using ProLong Gold (Life Technologies). Tissue was imaged

347 with 20x or 63x objectives, using a Zeiss Axio Observer.Z1 (Zeiss) fluorescent microscope with
348 Colibri.2 LED light source, an Apotome.2 (Zeiss) for optical sectioning, and an ORCA-R^2 digital
349 CCD camera (Hamamatsu).

350 *Image analysis.* Volocity image analysis software was used to quantify microcolony
351 areas. Image J was used to quantify the signal intensity of each channel at the centroid and
352 periphery of each microcolony, to generate relative signal intensities of fluorescent reporters.
353 Thresholding was used to define the area of each microcolony, the centroid was calculated, and
354 0.01 $pixel^2$ squares were selected to calculate values at the centroid. Peripheral measurements
355 depict bacteria in contact with host cells.

356

357 **Author Contributions.** Designed and performed experiments: KMD, JK, SC.
358 Intellectual/conceptual contribution: KMD, RRI. Analyzed the data: KMD, JK, SC, RRI. Wrote
359 the paper: KMD, RRI.

360

361 **Acknowledgments.** We thank the members of the Isberg lab, who provided valuable
362 advice and feedback throughout this project. We also thank the members of the Davis lab, who
363 provided feedback and suggestions during the final steps of manuscript preparation. The authors
364 of this manuscript declare no conflicts of interest. This work was supported by NIAID award
365 R01 AI110684 as well as by an American Cancer Society-Ellison Foundation Postdoctoral
366 Fellowship (PF-13-360-01-MPC), and a NIAID K22 Career Transition Award (1K22AI123465-
367 01).

368

369 **Figure Legends:**

370 **<u>Figure 1</u>: *ytfE* expression is regulated by NsrR and occurs within peripheral cells.** A)
371 C57BL/6 mice were inoculated intravenously (i.v.) with 10^3 WT *Y. pseudotuberculosis*, and
372 spleens were harvested at day 3 post-inoculation (PI). Bacterial transcripts were isolated from
373 splenic tissue, transcript levels were quantified by qRT-PCR relative to 16S, and the fold
374 increase in *ytfE* transcript levels is shown relative to the inoculum. Each dot represents an
375 individual mouse. B) Nitrogen stress was induced (NO_2, +) in cultures of WT and Δ*nsrR* strains,
376 and compared to untreated cultures (NO_2, -). The *ytfE* transcript levels are expressed relative to
377 16S, fold increase is relative to the average level in untreated WT cultures. Each column: 5
378 biological replicates, mean and SEM. C) C57BL/6 mice were inoculated i.v. with the WT
379 *hmp::mCherry ytfE::gfp* strain or the WT *yopE::mCherry ytfE;::gfp* strain, and spleens were
380 harvested at day 3 PI for fluorescence microscopy. Fluorescent signal intensity was determined
381 within the same peripheral and centroid cells for *hmp* and *ytfE* reporters or *yopE* and *ytfE*
382 reporters, and divided to generate the periphery/centroid ratio (4 mice/group). Dots: individual
383 microcolonies. D) Representative image of *hmp::mCherry* and *ytfE::gfp* reporters (top panels) or
384 *yopE::mCherry* and *ytfE::gfp* reporters (bottom panels); merge and single channel images are
385 shown. Scale bars: 20µm. Statistics: Wilcoxon matched pairs, **$p<0.01$, n.s.: not significant.
386

387 **<u>Figure 2</u>: *ytfE* contributes to growth in the spleen.** A) Co-infection with the WT and Δ*ytfE*
388 strains. C57BL/6 mice were inoculated i.v. with an equal mixture of $mCherry^+$ (*yopE::mCherry*)
389 WT and GFP^+ Δ*ytfE* strains, and spleens were harvested at day 3 PI. Competitive index: ratio of
390 Δ*ytfE*/WT CFUs in spleen at day 3, divided by ratio of Δ*ytfE*/WT CFUs in the inoculum. Dots:
391 individual mice. Dotted line: equal fitness, replicates completed on two separate days. B) WT

392 and Δ*ytfE* microcolony areas (μm^2) from the co-infection in panel 2A quantified (Experimental
393 Procedures) in 11 mice. C) C57BL/6 mice were inoculated i.v. with the WT GFP$^+$
394 *hmp::mCherry* or Δ*ytfE* GFP$^+$ *hmp::mCherry* strains, and spleens were harvested at day 3 PI for
395 fluorescence microscopy. Reporter signals were quantified within peripheral and centroid cells,
396 *hmp* reporter signal was divided by GFP. D) Representative image of a Δ*ytfE* GFP$^+$
397 *hmp::mCherry* microcolony, stained with Hoechst to detect host nuclei; merge and *hmp* single
398 channel images are shown Statistics: A): Wilcoxon Signed Rank Test, compared to a value of 1,
399 B): Mann-Whitney, C): Wilcoxon matched pairs, *p<0.05, ***p<0.001.
400
401 **Figure 3: Δ*ytfE* contributes to survival in the absence of *hmp*.** A) C57BL/6 mice were
402 inoculated i.v. with an equal mixture of *hmp* GFP$^+$ and Δ*hmp* Δ*ytfE* GFP$^+$ P_{hmp}*::mCherry* strains,
403 and spleens were harvested at day 3 PI. Competitive index: ratio of Δ*hmp* Δ*ytfE*/Δ*hmp* CFUs in
404 spleen at day 3, divided by ratio of Δ*hmp* Δ*ytfE*/Δ*hmp* CFUs in the inoculum. Dots: individual
405 mice. Dotted line: represents equal fitness. Statistics: Wilcoxon Signed Rank Test, compared to
406 a value of 1, n.s.: not significant. B) Total CFUs in the spleen during co-infection, when CI was
407 less than 1 (Δ*hmp* wins) or above or equal to 1 (Δ*hmp* Δ*ytfE* wins). Dots: individual mice. C)
408 Δ*hmp* and Δ*hmp* Δ*ytfE* microcolony areas (μm^2) from the co-infection quantified (Experimental
409 Procedures) in 10 mice. Dots: individual microcolonies. D) Reporter signals were quantified
410 within peripheral and centroid cells in the Δ*hmp* Δ*ytfE* strain during co-infection, *hmp* reporter
411 signal was divided by GFP. Dots: individual microcolonies. Statistics: B) and C): Mann-
412 Whitney, D): Wilcoxon matched pairs, *p<0.05, **p<0.01, n.s.: not significant.
413

414 **<u>Figure 4</u>: *ytfE* has limited effects on NO sensitivity in the absence of *hmp*.** A) Optical density
415 (A_{600nm}) was measured every 2 hours (time, hrs) within cultures of the indicated strains during
416 incubation in LB pH5.5 in the presence (+NO_2) and absence of $NaNO_2$. Data represents two
417 independent experiments. B) Optical density (A_{600nm}) was measured every 2 hours (time, hrs)
418 within cultures of the indicated strains during incubation in M9 minimal media in the presence
419 (+NO) and absence of the DETANONOate NO donor. Data represents three independent
420 experiments. C) C57BL/6 mice were inoculated i.v. with the Δ*ytfE* GFP^+ P_{hmp}*::mCherry* or
421 Δ*hmp* Δ*ytfE* GFP^+ P_{hmp}*::mCherry* strains, and spleens were harvested at day 3 PI for fluorescence
422 microscopy. Reporter signals were quantified within peripheral and centroid cells, *hmp* reporter
423 signal was divided by GFP. Dots: individual microcolonies. D) Representative images of Δ*ytfE*
424 and Δ*hmp* Δ*ytfE* microcolonies; merge and *hmp* single channel images are shown. Statistics:
425 Wilcoxon matched pairs, *$p<0.05$, n.s.: not significant.
426
427 **<u>Figure 5:</u> Rescue of *ytfE* restores fitness of the Δ*ytfE* strain.** A) C57BL/6 mice were
428 inoculated i.v. with an equal mixture of *ytfE* rescued GFP^+ and WT $mCherry^+$ strains, and spleens
429 were harvested at day 3 PI. Competitive index: ratio of *ytfE* rescue/WT CFUs in spleen at day 3,
430 divided by ratio of *ytfE* rescue/WT CFUs in the inoculum. Dots: individual mice. Dotted line:
431 equal fitness, replicates completed on two separate days. Statistics: Wilcoxon Signed Rank Test,
432 compared to a value of 1, n.s.: not significant. B) WT and *ytfE* rescue microcolony areas (μm^2)
433 from the co-infection quantified (Experimental Procedures) in 10 mice. Dots: individual
434 microcolonies. C) Representative images of WT $mCherry^+$ and *ytfE* rescued GFP^+ microcolonies.
435 Scale bar: 20µm. Statistics: Mann-Whitney, n.s.: not significant.

436 **References**

437 1. Bogdan C. Nitric oxide and the immune response. Nat Immunol. 2001;2(10):907-16.

438 2. Nathan C. Nitric oxide as a secretory product of mammalian cells. FASEB J.
439 1992;6(12):3051-64.

440 3. Pervin S, Singh R, Hernandez E, Wu G, Chaudhuri G. Nitric oxide in physiologic
441 concentrations targets the translational machinery to increase the proliferation of human breast
442 cancer cells: involvement of mammalian target of rapamycin/eIF4E pathway. Cancer Res.
443 2007;67(1):289-99.

444 4. Pervin S, Singh R, Chaudhuri G. Nitric oxide-induced cytostasis and cell cycle arrest of a
445 human breast cancer cell line (MDA-MB-231): potential role of cyclin D1. Proc Natl Acad Sci.
446 2001;98(6):3583-8.

447 5. Dubey M, Nagarkoti S, Awasthi D, Singh A, Chandra T, Kumaravelu J, et al. Nitric
448 oxide-mediated apoptosis of neutrophils through caspase-8 and caspase-3-dependent mechanism.
449 Cell Death Dis. 2016;7(9):e2348.

450 6. Kumar S, Barthwal M, Dikshit M. Cdk2 nitrosylation and loss of mitochondrial potential
451 mediate NO-dependent biphasic effect on HL-60 cell cycle. Free Radic Biol Med.
452 2010;48(6):851-61.

453 7. Kobayashi Y. The regulatory role of nitric oxide in proinflammatory cytokine expression
454 during the induction and resolution of inflammation. J Leukoc Biol. 2010;88(6):1157-62.

455 8. Zeigler M, Doseff A, Galloway M, Opalek J, Nowicki P, Zweier J, et al. Presentation of
456 nitric oxide regulates monocyte survival through effects on caspase-9 and caspase-3 activation. J
457 Biol Chem. 2003;278(15):12894-902.

458 9. Pautz A, Art J, Hahn S, Nowag S, Voss C, Kleinert H. Regulation of the expression of
459 inducible nitric oxide synthase. Nitric Oxide. 2010;23(2):75-93.

460 10. Fang F. Perspective series: host/pathogen interactions. Mechanisms of nitric oxide-
461 related antimicrobial activity. J Clin Invest. 1997;99(12):2818-25.

462 11. Pullan S, Gidley M, Jones R, Barrett J, Stevanin T, Read R, et al. Nitric oxide in
463 chemostat-cultured *Escherichia coli* is sensed by Fnr and other global regulators: unaltered
464 methionine biosynthesis indicates lack of S nitrosation. J Bacteriol. 2007;189(5):1845-55.

465 12. Gilberthorpe N, Lee M, Stevanin T, Read R, Poole R. NsrR: a key regulator
466 circumventing *Salmonella enterica* serovar Typhimurium oxidative and nitrosative stress *in vitro*
467 and in IFN-gamma-stimulated J774.2 macrophages. Microbiology. 2007;153(6):1756-71.

468 13. Overton T, Justino M, Li Y, Baptista J, Melo A, Cole J, et al. Widespread distribution in
469 pathogenic bacteria of di-iron proteins that repair oxidative and nitrosative damage to iron-sulfur
470 clusters. J Bacteriol. 2008;190(6):2004-13.

471 14. Bodenmiller D, Spiro S. The yjeB (nsrR) gene of *Escherichia coli* encodes a nitric oxide-
472 sensitive transcriptional regulator. J Bacteriol. 2006;188(3):874-81.

473 15. Tucker N, Hicks M, Clarke T, Crack J, Chandra G, Le Brun N, et al. The transcriptional
474 repressor protein NsrR senses nitric oxide directly via a [2Fe-2S] cluster. PLoS ONE.
475 2008;3(11):e3623.

476 16. Volbeda A, Dodd E, Darnault C, Crack J, Renoux O, Hutchings M, et al. Crystal
477 structures of the NO sensor NsrR reveal how its iron-sulfur cluster modulates DNA binding. Nat
478 Commun. 2017;8:15052.

479 17. Filenko N, Spiro S, Browning D, Squire D, Overton T, Cole J, et al. The NsrR regulon of
480 *Escherchia coli* K-12 includes genes encoding the hybrid cluster protein and the periplasmic,
481 respiratory nitrite reductase. J Bacteriol. 2007;189(12):4410-7.

482 18. Partridge J, Bodenmiller D, Humphrys M, Spiro S. NsrR targets in the *Escherchia coli*
483 genome: new insights into DNA sequence requirements for binding and a role for NsrR in the
484 regulation of motility. Mol Microbiol. 2009;73(4):680-94.

485 19. Robinson J, Brynildsen M. A kinetic platform to determine the fate of nitric oxide in
486 *Escherichia coli*. PLoS Comput Biol. 2013;9(5):e103049.

487 20. Poole R, Anjum M, Membrillo-Hernández J, Kim S, Hughes M, Stewart V. Nitric oxide,
488 nitrite, and Fnr regulation of *hmp* (flavohemoglobin) gene expression in *Escherichia coli* K-12. J
489 Bacteriol. 1996;178(18):5487-92.

490 21. Justino M, Almeida C, Gonçalves V, Teixeira M, Saraiva L. *Escherichia coli* YtfE is a
491 di-iron protein with an important function in assembly of iron-sulphur clusters. FEMS Microbiol
492 Lett. 2006;257(2):278-84.

493 22. Todorovic S, Justino M, Wellenreuther G, Hildebrandt P, Murgida D, Meyer-Klaucke W,
494 et al. Iron-sulfur repair YtfE protein from *Escherichia coli*: structural characterization of the di-
495 iron center. J Biol Inorg Chem. 2008;13(5):765-70.

496 23. Miller H, Kwuan L, Schwiesow L, Bernick D, Mettert E, Ramirez H, et al. IscR is
497 essential for *Yersinia pseudotuberculosis* type III secretion and virulence. PLoS Pathog.
498 2014;10(6):e1004194.

499 24. Miller H, Schwiesow L, Au-Yeung W, Auerbuch V. Hereditary hemochromatosis
500 predisposes mice to *Yersinia pseudotuberculosis* infection even in the absence of the type III
501 secretion system. Front Cell Infect Microbiol. 2016;6:69.

502 25. Schwiesow L, Mettert E, Wei Y, Miller H, Herrera N, Balderas D, et al. Control of *hmu*
503 heme uptake genes in *Yersinia pseudotuberculosis* in response to iron sources. Front Cell Infect
504 Microbiol. 2018;8:47.

505 26. Hubbert W, Petenyi C, Glasgow L, Uyeda C, Creighton S. *Yersinia pseudotuberculosis*
506 infection in the United States. Septicemia, appendicitis, and mesenteric lymphadenitis. Am J
507 Trop Med Hyg. 1971;20(5):679-84.

508 27. Gurry J. Acute terminal ileitis and yersinia infection. Br Med J. 1974;2(5913):264-6.

509 28. Capron J, Delamarre J, Delcenserie R, Gineston J, Dupas J, Lorriaux A. Liver absess
510 complicating *Yersinia pseudotuberculosis* ileitis. Gastroenterology. 1981;81(1):150-2.

511 29. Paff J, Triplett D, Saari T. Clinical and laboratory aspects of *Yersinia pseudotuberculosis*
512 infections, with a report of two cases. Am J Clin Pathol. 1976;66(1):101-10.

513 30. Barnes P, Bergman M, Mecsas J, Isberg R. *Yersinia pseudotuberculosis* disseminates
514 directly from a replicating bacterial pool in the intestine. J Exp Med. 2006;203(6):1591-601.

515 31. Crimmins G, Mohammadi S, Green E, Bergman M, Isberg R, Mecsas J. Identification of
516 MrtAB, an ABC transporter specifically required for *Yersinia pseudotuberculosis* to colonize the
517 mesenteric lymph nodes. PLoS Pathog. 2012;8(8):e1002828.

518 32. Davis K, Mohammadi S, Isberg R. Community behavior and spatial regulation within a
519 bacterial microcolony in deep tissue sites serves to protect against host attack. Cell Host
520 Microbe. 2015;17(1):21-31.

521 33. Zhang Y, Khairallah C, Sheridan B, van der Velden A, Bliska J. CCR2+ inflammatory
522 monocytes are recruited to *Yersinia pseudotuberculosis* pyogranulomas and dictate adaptive
523 responses at the expense of innate immunity during oral infection. Infect Immun.
524 2018;86(3):e00782-17.

525 34. Peterson L, Philip N, DeLaney A, Wynosky-Dolfi M, Asklof K, Gray F, et al. RIPK1-
526 dependent apoptosis bypasses pathogen blockage of innate signaling to promote immune
527 defense. J Exp Med. 2017;214(11):3171-82.

528 35. Durand E, Maldonado-Arocho F, Castillo C, Walsh R, Mecsas J. The presence of
529 professional phagocytes dictates the number of host cells targeted for Yop translocation during
530 infection. Cell Microbiol. 2010;12(8):1064-82.

531 36. Sebbane F, Lemaître N, Sturdevant D, Rebeil R, Virtaneva K, Porcella S, et al. Adaptive
532 response of *Yersinia pestis* to extracellular effectors of innate immunity during bubonic plague.
533 Proc Natl Acad Sci. 2006;103(31):11766-71.

534 37. Nuss A, Beckstette M, Pimenova M, Schmühl C, Opitz W, Pisano F, et al. Tissue dual
535 RNA-seq allows fast discovery of infection-specific functions and riboregulators shaping host-
536 pathogen transcriptomes. Proc Natl Acad Sci. 2017;114(5):E791-E800.

537 38. Karlinsey J, Bang I, Becker L, Frawley E, Porwollik S, Robbins H, et al. The NsrR
538 regulon in nitrosative stress resistance of *Salmonella enterica* serovar Typhimurium. Mol
539 Microbiol. 2012;85(6):1179-93.

540 39. Shepherd M, Achard M, Idris A, Totsika M, Phan M, Peters K, et al. The cytochrome bd-
541 I respiratory oxidase augments survival of multidrug-resistant *Escherichia coli* during infection.
542 Sci Rep. 2016;6:35285.

543 40. Shiloh M, MacMicking J, Nicholson S, Brause J, Potter S, Marino M, et al. Phenotype of
544 mice and macrophages deficient in both phagocyte oxidase and inducible nitric oxide synthase.
545 Immunity. 1999;10(1):29-38.

546 41. Vasquez-Torres A, Jones-Carson J, Mastroeni P, Ischiropoulos H, Fang F. Antimicrobial
547 actions of the NADPH phagocyte oxidase and inducible nitric oxide synthase in experimental

548 salmonellosis. I. Effects on microbial killing by activated peritoneal macrophages in vitro. J Exp
549 Med. 2000;192(2):227-36.

550 42. Shiloh M, Nathan C. Reactive nitrogen intermediates and the pathogenesis of *Salmonella*
551 and *Mycobacteria*. Curr Opin Microbiol. 2000;3(1):35-42.

552 43. Bang I, Liu L, Vasquez-Torres A, Crouch M, Stamler J, Fang F. Maintenance of nitric
553 oxide and redox homeostasis by the *Salmonella* flavohemoglobin *hmp*. J Biol Chem.
554 2006;281(38):28039-47.

555 44. Mashruwala A, Boyd J. The *Staphylococcus aureus* SrrAB regulatory system modulates
556 hydrogen peroxide resistance factors, which imparts protection to aconitase during aerobic
557 growth. PLoS ONE. 2017;12(1):e0170283.

558 45. Kinkel T, Roux C, Dunman P, Fang F. The *Staphylococcus aureus* SrrAB two-
559 component system promotes resistance to nitrosative stress and hypoxia. MBio.
560 2013;4(6):e00696-13.

561 46. Jang S, Imlay J. Micromolar intracellular hydrogen peroxide disrupts metabolism by
562 damaging iron-sulfur enzymes. J Biol Chem. 2007;282(2):929-37.

563 47. Justino M, Almeida C, Teixeira M, Saraiva L. *Escherichia coli* di-iron YtfE protein is
564 necessary for the repair of stress-damaged iron-sulfur clusters. J Biol Chem.
565 2007;282(14):10352-9.

566 48. Velayudhan J, Karlinsey J, Frawley E, Becker L, Nartea M, Fang F. Distinct roles of the
567 *Salmonella enterica* serovar Typhimurium CyaY and YggX proteins in the biosynthesis and
568 repair of iron-sulfur clusters. Infect Immun. 2014;82(4):1390-401.

569 49. Silva L, Baptista J, Batley C, Andrews S, Saraiva L. The di-iron RIC protein (YtfE) of
570 *Escherichia coli* interacts with the DNA-binding protein from starved cells (Dps) to diminish
571 RIC protein-mediated redox stress. J Bacteriol. 2018;200(24):e00527-18.

572 50. Djaman O, Outten F, Imlay J. Repair of oxidized iron-sulfur clusters in *Escherchia coli*. J
573 Biol Chem. 2004;279(43):44590-99.
574

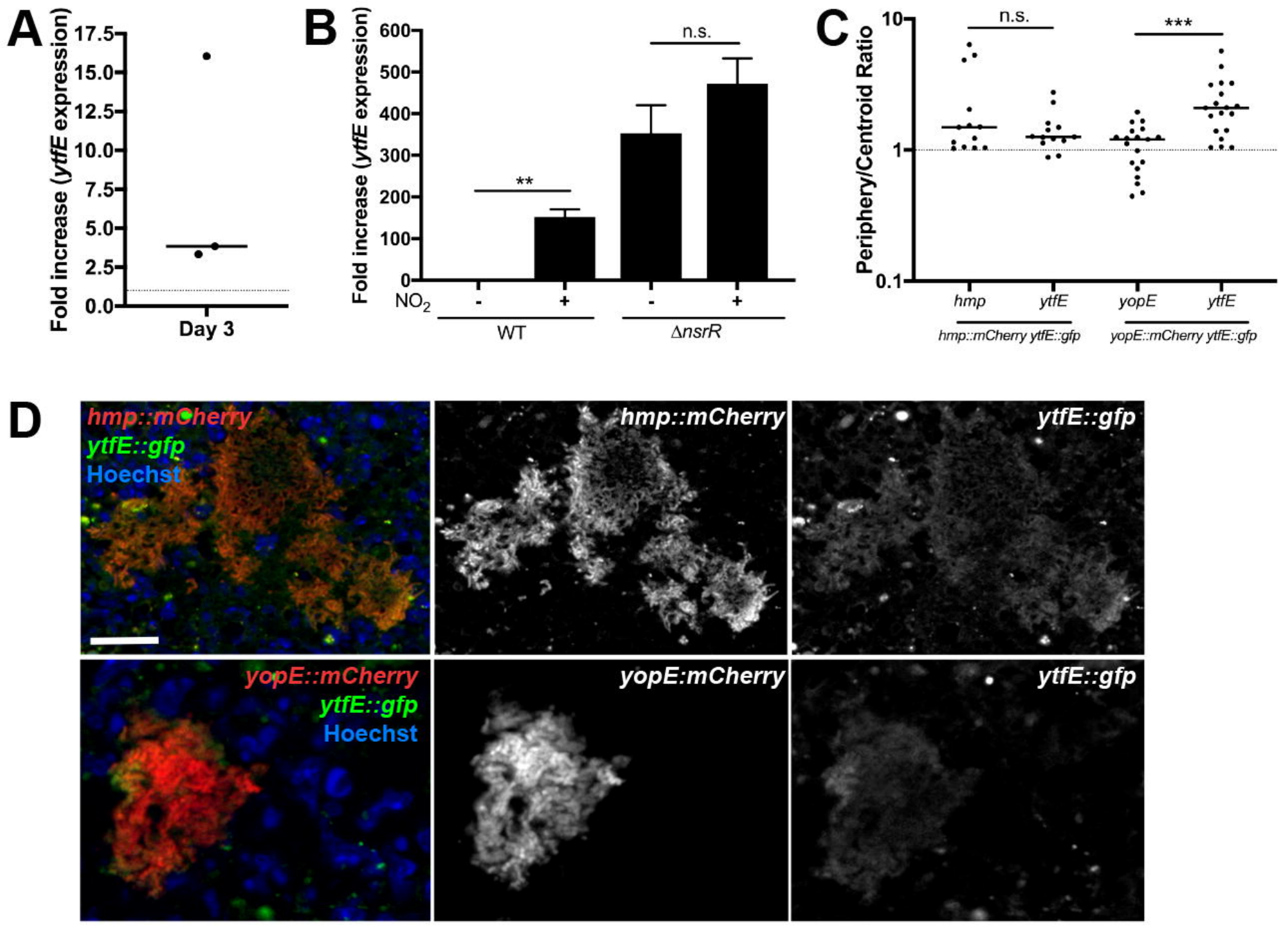
A
Fold increase (ytfE expression)
17.5
15.0
12.5
10.0
7.5
5.0
2.5
0.0
Day 3
B
Fold increase (ytfE expression)
600
500
400
300
200
100
0
n.s.
**
NO2
-
+
-
+
WT
ΔnsrR
C
Periphery/Centroid Ratio
10
1
0.1
n.s.
***
hmp
ytfE
yopE
ytfE
hmp::mCherry ytfE::gfp
yopE::mCherry ytfE::gfp
D
hmp::mCherry
ytfE::gfp
Hoechst
hmp::mCherry
ytfE::gfp
yopE::mCherry
ytfE::gfp
Hoechst
yopE:mCherry
ytfE::gfp

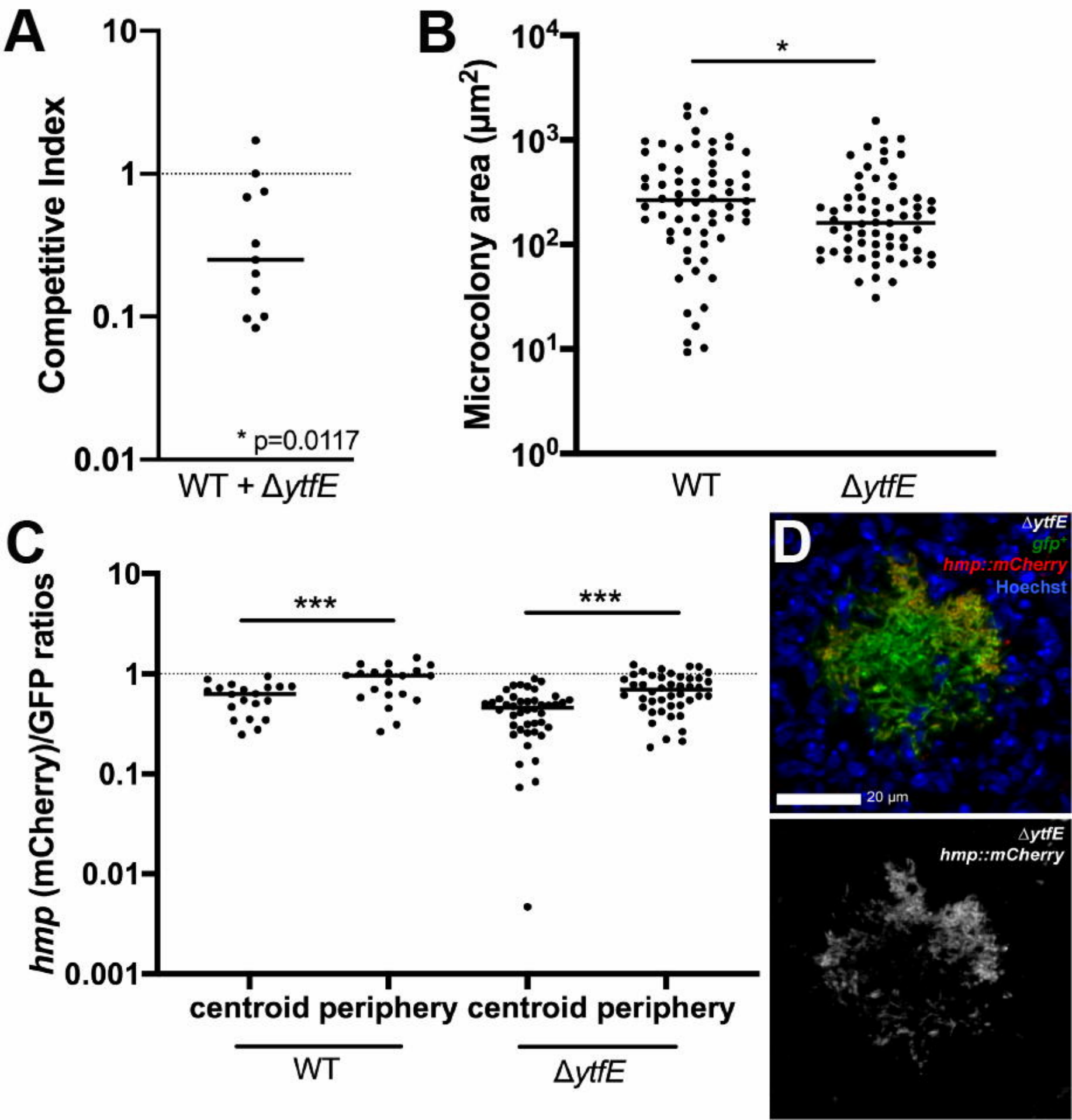
A
Competitive Index
10
1
0.1
0.01
* p=0.0117
WT + ΔytfE
B
Microcolony area (μm²)
10⁴
10³
10²
10¹
10⁰
*
WT
ΔytfE
C
hmp (mCherry)/GFP ratios
10
1
0.1
0.01
0.001
***
***
centroid periphery centroid periphery
WT
ΔytfE
D
ΔytfE
gfp⁺
hmp::mCherry
Hoechst
20 μm
ΔytfE
hmp::mCherry

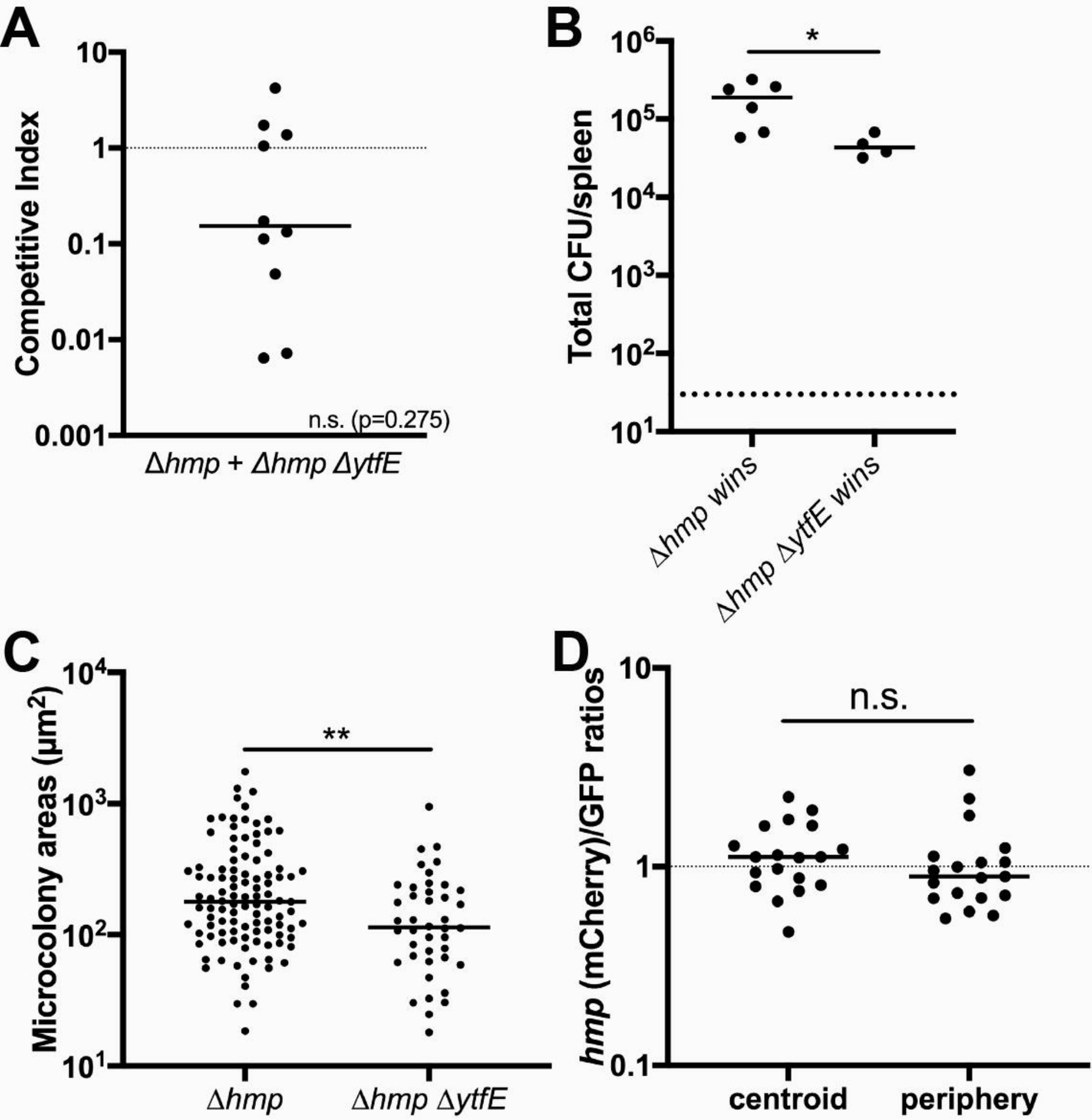
A
Competitive Index
10
1
0.1
0.01
0.001
n.s. (p=0.275)
Δhmp + Δhmp ΔytfE
B
Total CFU/spleen
10^6
10^5
10^4
10^3
10^2
10^1
*
Δhmp wins
Δhmp ΔytfE wins
C
Microcolony areas (μm^2)
10^4
10^3
10^2
10^1
**
Δhmp
Δhmp ΔytfE
D
hmp (mCherry)/GFP ratios
10
1
0.1
n.s.
centroid
periphery

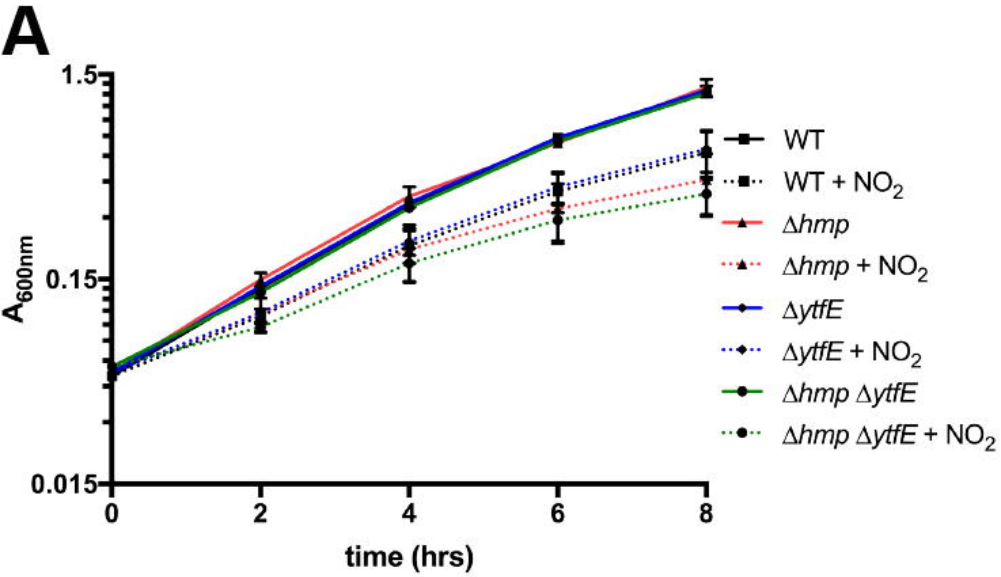
A
1.5
0.15
0.015
A_{600nm}
0
2
4
6
8
time (hrs)
WT
WT + NO_2
Δhmp
Δhmp + NO_2
ΔytfE
ΔytfE + NO_2
Δhmp ΔytfE
Δhmp ΔytfE + NO_2

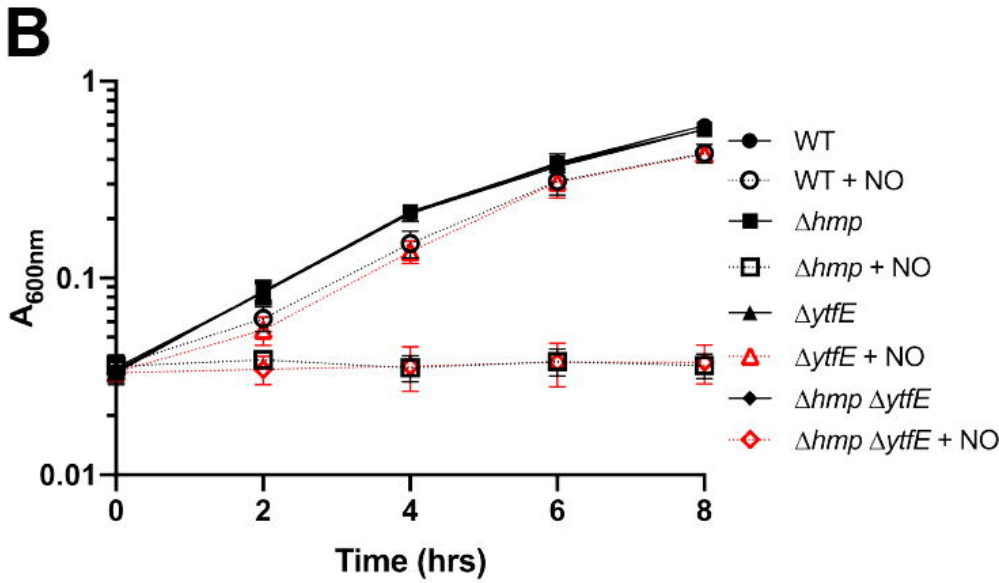
B
1
0.1
0.01
A_{600nm}
0
2
4
6
8
Time (hrs)
WT
WT + NO
Δhmp
Δhmp + NO
ΔytfE
ΔytfE + NO
Δhmp ΔytfE
Δhmp ΔytfE + NO

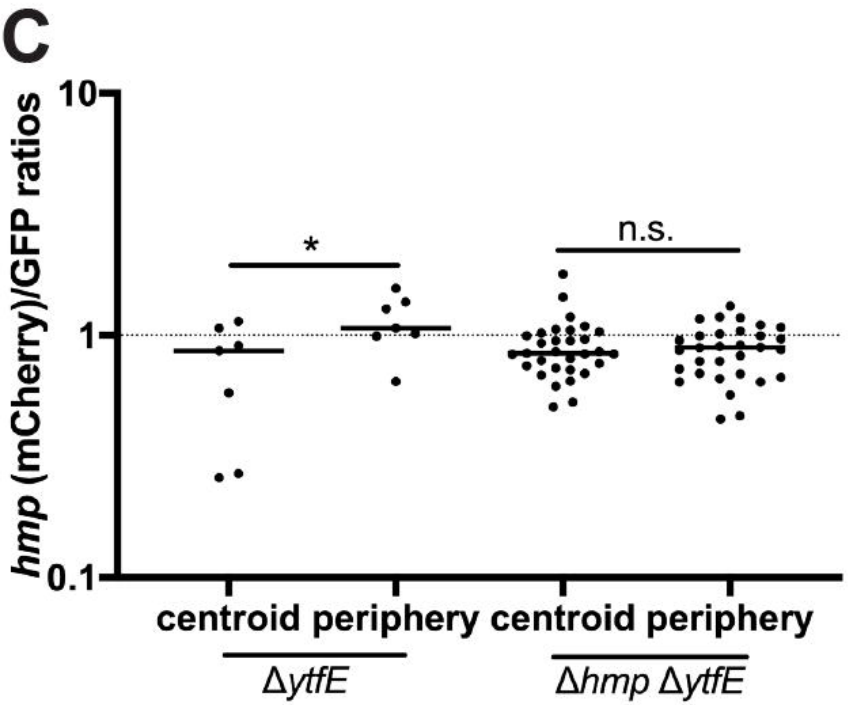
C
10
1
0.1
hmp (mCherry)/GFP ratios
*
n.s.
centroid
periphery
centroid
periphery
ΔytfE
Δhmp ΔytfE

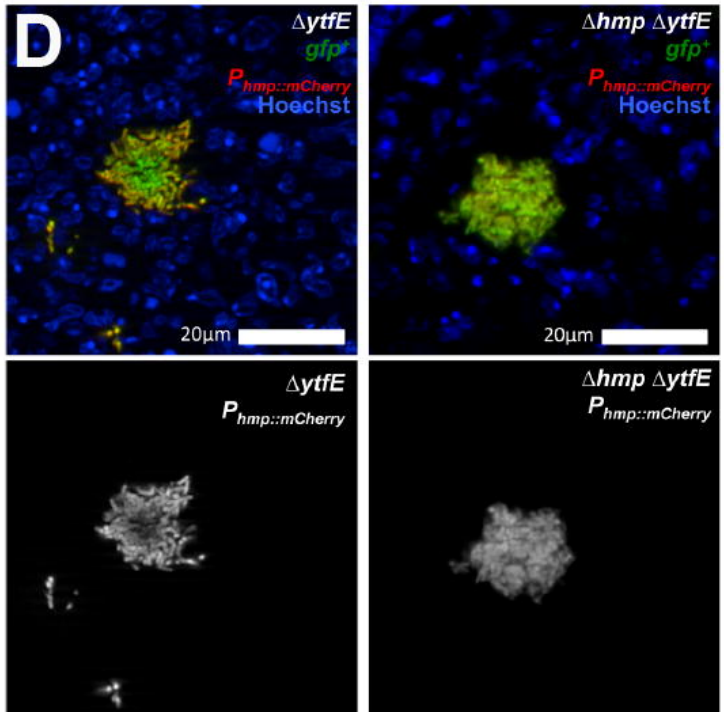
D
ΔytfE
gfp+
$P_{hmp::mCherry}$
Hoechst
20µm
Δhmp ΔytfE
gfp+
$P_{hmp::mCherry}$
Hoechst
20µm
ΔytfE
$P_{hmp::mCherry}$
Δhmp ΔytfE
$P_{hmp::mCherry}$

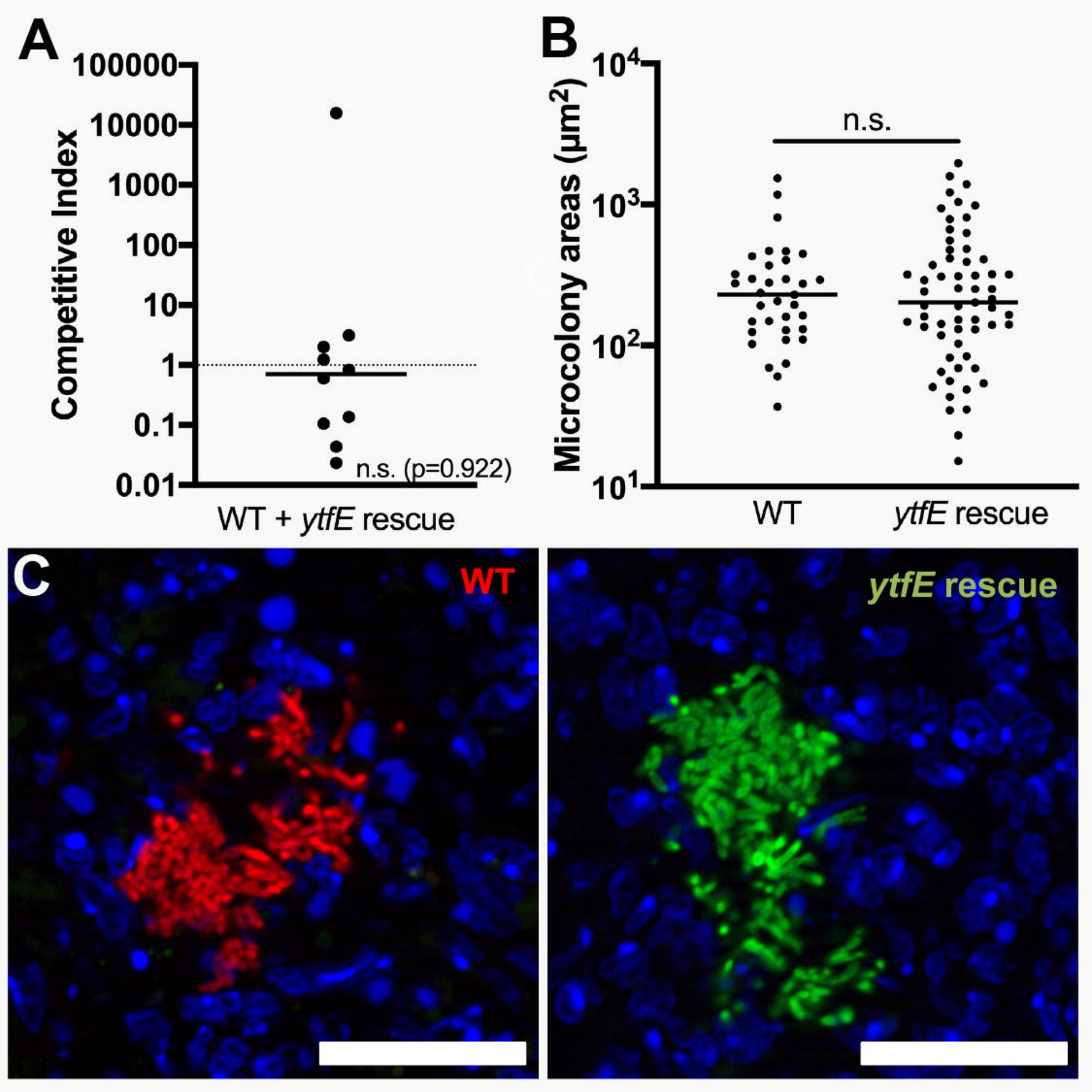
A
Competitive Index
100000
10000
1000
100
10
1
0.1
0.01
n.s. (p=0.922)
WT + ytfE rescue
B
Microcolony areas (μm²)
10⁴
10³
10²
10¹
n.s.
WT
ytfE rescue
C
WT
ytfE rescue